Organic & Biomolecular Chemistry

Cite this: DOI: 10.1039/c2ob26393a

www.rsc.org/obc

PAPER

Synthesis, antibacterial activity and mode of action of novel linoleic acid–dipeptide–spermidine conjugates†

Seema Joshi,‡[a,b] Rikeshwer P. Dewangan,‡[a] Shruti Yadav,[a] Diwan S. Rawat[b] and Santosh Pasha*[a]

Received 18th July 2012, Accepted 4th September 2012
DOI: 10.1039/c2ob26393a

Towards therapeutically viable mimics of host defense cationic peptides (HDCPs) here we report the design and synthesis of a small library, based on a novel hydrophobic–dipeptide–spermidine template. Lipidated sequences **11**, **14**, **15**, **16**, **18** and **19** exhibited potent activity against susceptible as well as drug resistant Gram-positive and Gram-negative bacterial strains. Structure–activity relationships of the template revealed a hydrophobicity window of 50–70% with minimum +2 charges to be crucial for activity and cell selectivity. Active sequences **14**, **15** and **16** exhibited different modes of action based on dipeptide composition as revealed by studies on model membranes, intact bacterial cells and DNA. Further, severe damage to surface morphology of methicillin resistant *S. aureus* caused by **14**, **15** and **16** at 10 × MIC was observed. The present study provides us two active sequences (**14** and **16**) with a membrane perturbing mode of action, cell selectivity to hRBCs and keratinocytes along with potent activity against clinically relevant pathogen MRSA. The designed template thus may prove to be a suitable probe to optimize sequences for better selectivity and potential to combat a wide range of drug resistant strains in further research.

Introduction

The emergence of multiple drug resistant bacterial strains causes millions of deaths worldwide.[1,2] The rise in morbidity and mortality related to microbial infections has led to tremendous pressure on health care systems.[3] Host defense cationic peptides (HDCPs) are known for their wide range of activity against microorganisms including bacteria, fungi, viruses and even cancerous cells. With multifaceted roles in innate immunity and a direct cell lytic mode of action, it is difficult for a microorganism to endure resistance against HDCPs.[4,5] Therefore HDCPs are being explored as promising alternatives to conventional drugs.[6,7]

However in spite of all these advantages only a handful of antimicrobial peptides are under clinical trials due to their high manufacturing costs, poor pharmacokinetic properties and associated toxicity issues.[8] To address these issues, efforts are being made to explore the characteristic features of HDCPs such as net positive charge at physiological pH and hydrophobic bulk[9] to develop more economic membrane active antimicrobial peptidomimetics. Many classes of compounds such as ceragenins,[10,11] oligoacyllysines,[12,13] arylamides,[14] peptoid based scaffolds[15] and lipopeptides[16,17] that mimic HDCPs are being developed as alternative antimicrobial agents with low susceptibility for development of resistance.

Cationic polyamines spermine, spermidine and putrescine are ubiquitous components of eukaryotic and prokaryotic cells with multiple roles in modulating functions of DNA, RNA and proteins inside the cells.[18] A number of modified/conjugated polyamines have been reported with various biological activities such as LPS sequestration,[19] anti-parasitic activity,[20,21] anticancer activity,[22,23] as well as nucleic acid carriers for DNA transfection.[24] Considering the medicinal potential of polyamines we anticipated that incorporation of spermidine as a positively charged moiety to hydrophobic–dipeptides may lead to small peptidomimetics with better antibacterial activity.

Long-chain free fatty acids (FFAs) are known to be present at skin surfaces, maintaining an acidic pH which helps to prevent colonization of various microorganisms including methicillin-resistant *S. aureus* and *H. pylori*.[25–27] The mode of bacterial killing for FFAs has not been unambiguously determined however, the prime target is believed to be microbial membranes where direct lysis, perturbation of the electron transport chain, oxidative phosphorylation and inhibition of fatty acid metabolism have been reported as some of the probable causes leading to bacterial cell death.[28,29] Therefore with multiple non-specific modes of action, a broad range of activity and minimum toxicity long chain FFAs were chosen to be incorporated into designed peptidomimetics as the hydrophobic moiety.

[a]*Institute of Genomics and Integrative Biology, Mall Road, Delhi, India. E-mail: spasha@igib.res.in; Fax: +91 11 27667471; Tel: +91 11 27666156*
[b]*Department of Chemistry, University of Delhi, Delhi, India*
† Electronic supplementary information (ESI) available: HPLC traces, mass spectra and ^{1}H NMR data of representative designed sequences. See DOI: 10.1039/c2ob26393a
‡ These authors have contributed equally to the work.

Here we report the design and synthesis of a small library of hydrophobic–dipeptide–spermidine template based sequences consisting of cationic polyamine spermidine and FFAs (linoleic acid and stearic acid). We dissected the template into two parts to evaluate the role of the hydrophobic moiety–dipeptide or cationic–dipeptide part of the template in imparting activity and/or selectivity to these sequences. We further evaluated interaction of the active sequences with model membranes, intact bacterial cells and DNA to probe into the molecular mode of action.

Results and discussion

1. Design and synthesis

Clinically approved lipopeptide antibiotics such as polymyxin B, daptomycin and echinocandins have spurred the research for novel analogues of these classes of lipopeptides with clinical relevance.[30–32] A large number of membrane active lipopeptides have been designed to achieve net positive charge (at least +2) and hydrophobic bulk making use of varied chemical moieties.[15–17] However, cationic lipopeptides with saturated fatty acids are difficult to optimize for cell selectivity.[33] Realizing the importance of charge and amphiphilicity for membrane active antimicrobial peptidomimetics, we designed a novel short template that comprised a hydrophobic moiety attached at the N-terminus to dipeptide–spermidine. The sequences presented in the current study are unique where inherently active unsaturated fatty acids were coupled to dipeptides which were further tagged with organic polyamine spermidine, prompting membrane activity as well as cellular translocation to bind DNA. For the dipeptide portion we made use of three different combinations of tryptophan (Trp) and ornithine (Orn) amino acids *i.e.* Trp–Trp, Trp–Orn and Orn–Orn. Hydrophobic Trp amino acid was chosen because of its well documented membrane anchoring property.[34] Cationic residue Orn was used to impart protease stability to designed sequences due to its non-ribosomal origin. Based on various biological activities associated with spermidine conjugates as outlined above, we incorporated spermidine at the C-terminus of the dipeptides to give rise to sequences **1–3** (Table 1). N-Terminal hydrophobic tagging of dipeptide sequences was done to evaluate the role of FFAs such as linoleic acid and stearic acid in imparting activity leading to sequences **4–11**. To evaluate the role of lipidation as a control an aromatic moiety 3-(4-hydroxyphenyl)-propionic acid (HPPA) was also conjugated. The HPPA was used based on our observations that covalent hybridization of HPPA to a tetra-peptide template led to the discovery of some potent tetra-peptidomimetics.[35] To have an appropriate balance between charge and hydrophobicity, the designed complete template consisting of a hydrophobic tag at the N-terminal with cationic spermidine at the C-terminus resulting in sequences **12–19** was also synthesized. With at least +2 charge and varied degrees of hydrophobicity these conjugates were further evaluated for antibacterial activity and mode of action studies.

The sequences were synthesized using a combination of solid phase and solution phase strategy as presented in Scheme 1. Structures of representative sequences are shown in Fig. 1.

2. Antibacterial activity

Antibacterial activity of designed sequences against a range of Gram-positive and Gram-negative bacterial strains was determined using the serial broth dilution method (Table 2). Out of the sequences **1–3**, sequence **1** exhibited MIC at 113.6 μg mL^{-1} against *S. aureus*. Out of sequences **4–11**, **4**, **5** and **9** were devoid of antibacterial activity, whereas sequences **6** and **7** showed MIC at 113.6 μg mL^{-1} against *S. aureus* and *B. subtilis*. Sequence **8** with +1 charge showed moderate activity against tested strains with MIC in the range of 28.4–113.6 μg mL^{-1}. Sequence **11** with +1 charge and stearic acid tagging showed

Table 1 Sequences, molecular mass, charge and % of acetonitrile at RP-HPLC elution

		Mass $[M]^+$			
Sequences	Composition	Calc.	Obser.	Charge	% acetonitrile at RP-HPLC elution
1	NH_2-WW-spermidine	518.3238	518.3228	+3	26
2	NH_2-WO-spermidine	446.3238	446.3226	+4	22
3	NH_2-OO-spermidine	374.3238	374.3235	+5	19
4	HPPA-WW-COOH	539.2289	539.2277	−1	61
5	HPPA-WO-COOH	467.2289	467.2278	0	46
6	LIN-WW-COOH	653.4061	653.62[a]	−1	84
7	LIN-WO-COOH	581.4061	581.4063	0	79
8	LIN-OO-COOH	509.4061	509.4054	+1	59
9	STER-WW-COOH	657.4374	657.68[a]	−1	88
10	STER-WO-COOH	585.4374	585.4366	0	89
11	STER-OO-COOH	513.4374	513.4368	+1	70
12	HPPA-WW-spermidine	666.3762	666.3762	+2	52
13	HPPA-WO-spermidine	594.3762	594.3760	+3	27
14	LIN-WW-spermidine	780.5535	780.5537	+2	70
15	LIN-WO-spermidine	708.5535	708.5544	+3	62
16	LIN-OO-spermidine	636.5535	636.5540	+4	51
17	STER-WW-spermidine	784.5848	784.5858	+2	76
18	STERWO-spermidine	712.5848	712.5847	+3	68
19	STER-OO-spermidine	640.5848	640.5853	+4	63

HPPA: 3-(4-hydroxy phenyl)-propionic acid; LIN: linoleic acid; STER: stearic acid.[a] ESI-MS data.

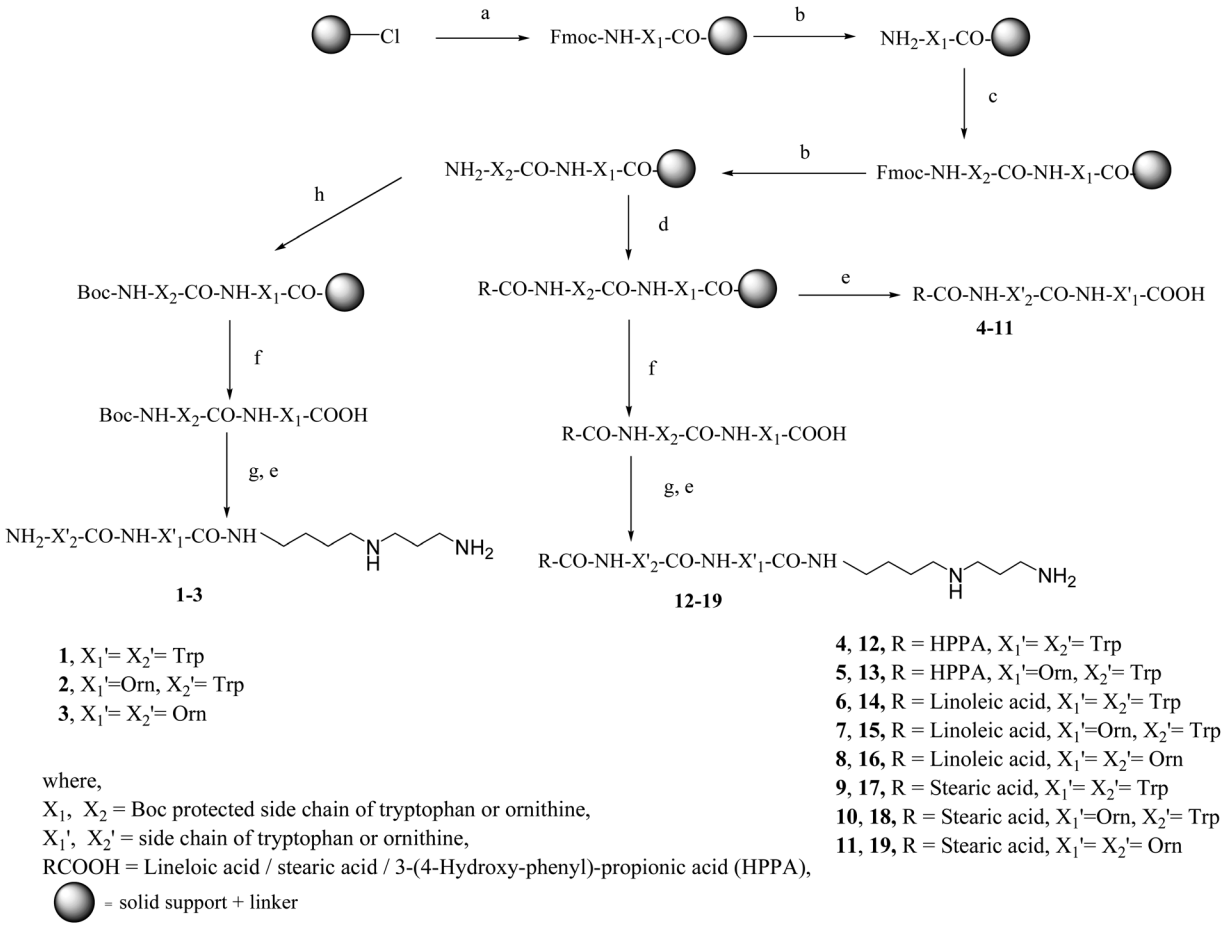

Scheme 1 Reagents and conditions: (a) Fmoc-NH-X_1-COOH, DIPEA, DCM : DMF (50 : 50), 3 h, MeOH for 30 min, (b) 20% piperidine in DMF, (c) Fmoc-NH-X_2-COOH, HOBt, DIPCDI, DCM : DMF (50 : 50), 1.5 h, (d) R-COOH, HOBt, DIPCDI, DCM : DMF (50 : 50), 14 h, (e) 50% TFA–DCM, (f) TFE : acetic acid : DCM (1 : 1 : 8), 1.5 h, (g) N^1,N^4-bis(Boc)-spermidine, DIPCDI, HOBt, THF, 0 °C for 30 min, rt 18 h, (h) $(Boc)_2O$, DIPEA–DCM, 1.5 h.

good antibacterial activity against Gram-positive bacterial strains with MIC in the range of 7.1–14.2 μg mL^{-1}. Sequence **12** with HPPA tagging showed moderate activities against almost all the tested strains with MIC in the range of 56.8–113.6 μg mL^{-1}. Sequence **13** showed activity against *S. aureus* and *B. subtilis* with MIC at 113.6 μg mL^{-1}. Percentage of acetonitrile from RP-HPLC elution profile data as an indicator for hydrophobicity along with MIC data showed that the designed sequences with a threshold of acetonitrile (50%) with a single positive charge (**8** and **11**) showed good antibacterial activity (Table 2). Therefore similar to the previously reported concept of a hydrophobicity window for HDCPs,[36] here we propose a window of 50% to 70% acetonitrile at RP-HPLC elution (Table 1), below or above this threshold the sequences were either less active or inactive. MIC data on these sequences thus ensured that lipidation with a single positive charge may lead to activity (**8** and **11**) however; charge alone (**1–3**) without lipidation is not sufficient to impart appreciable activity.

Sequences **14–19** showed a broad range of activity against Gram-positive as well as Gram-negative bacterial strains with MIC values in the range of 0.88–28.4 μg mL^{-1}. Against *E. coli* and *P. aeruginosa*, MIC values of these sequences were found to be in the range of 3.5–28.4 μg mL^{-1} and 7.1–14.2 μg mL^{-1} respectively (except sequence **17**). Against the four Gram-positive strains tested in the study, all the sequences showed MIC values below 15 μg mL^{-1}. Interestingly MIC of these sequences against MRSA was found to be comparable or even better as compared to *S. aureus*. Sequence **17** with 76% acetonitrile at RP-HPLC elution was above the hydrophobicity threshold of 70%, above which the sequences were found to be less active against tested strains. It is important to note that in comparison to standard antibiotics tetracycline and polymyxin B, sequences **14–19** showed better MIC against MRSA (except **17**), where **14** and **15** were very promising with MIC at 0.88 μg mL^{-1}.

3. Toxicity evaluation of designed sequences

The efficacy of designed sequences as safe antibacterial agents was established based on their interaction with enucleated hRBCs and human keratinocytes (HaCaT cells). Most of the sequences (**1–7**, **9**, **12**, **13**, **16** and **17**) were found to be non-hemolytic up to 62.5 μg mL^{-1}. Sequences **8** and **11** were found to be lytic to hRBCs, however on conjugation of spermidine,

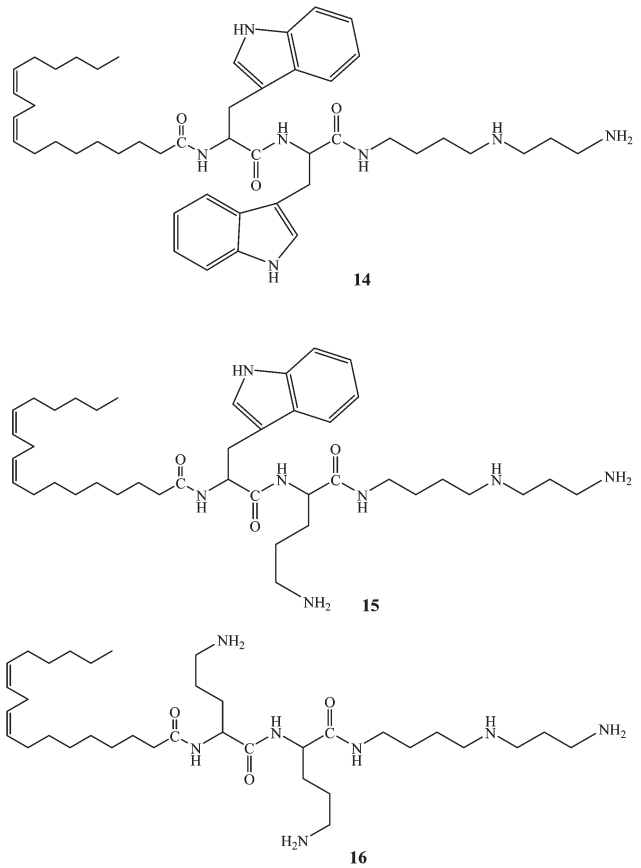

Fig. 1 Representative structures of designed antibacterial sequences.

reduction in hemolysis was observed for N-terminal tagged dipeptides (Table 2). Sequences **14** and **16** showed negligible hemolytic activity whereas sequence **15** caused 40% hemolysis at concentrations corresponding to 18–78 times its MIC values against Gram-positive bacterial strains tested in the study. Sequences with stearic acid tagging (**18** and **19**) were found to be more lytic to hRBC than the linoleic acid counter sequences (**15** and **16**). Similar to our results, experimental evidence is present in the literature that reports cationic lipopeptides with saturated fatty acid chain length to be more lytic as compared to their unsaturated counterparts.[33]

Since HDCP mimics are considered more suitable as topical agents, we evaluated the effects of designed sequences on human keratinocytes. Results of the MTT assay on HaCaT cells showed 80% and 100% cell survival for sequences **14** and **16** at 62.5 μg mL^{-1} respectively (Fig. 2). Even up to a high concentration of 250 μg mL^{-1} 65% and 78% cell survival was observed for sequences **14** and **16** respectively. These data thus confirm no detrimental effects of these sequences on human keratinocytes even upon incubation for 18 h.

4. Bactericidal kinetics

HDCPs with a predominant membrane active mode of action are endowed with the potential to kill bacterial cells within minutes at concentrations higher than MIC. In order to monitor the rapidity of mode of action of designed sequences, we incubated sequences **14**, **15** and **16** with log-phase MRSA at 37 °C and monitored the course of change in optical density (OD_{600}) at different time intervals. The results showed inhibition of bacterial growth after 2 h at MIC for sequences **15** and **16** (Fig. 3).

Table 2 Antibacterial activity and hemolysis of designed sequences against Gram-positive and Gram-negative bacterial strains

	MIC (μg mL^{-1})							
	Gram-negative bacteria			Gram-positive bacteria				
Sequences	*E. coli*	*P. aeruginosa*	*A. baumannii*	*S. aureus*	*E. faecalis*	*B. subtilis*	MRSA	% hemolysis (at 62.5 μg mL^{-1})
1	>227.2	ND	ND	113.6	ND	ND	ND	0
2	>227.2	ND	ND	>227.2	ND	ND	ND	0
3	>227.2	ND	ND	>227.2	ND	ND	ND	0
4	>227.2	>227.2	>227.2	>227.2	>227.2	>227.2	>227.2	0
5	>227.2	>227.2	>227.2	>227.2	>227.2	>227.2	>227.2	0
6	>227.2	>227.2	>227.2	113.6	>227.2	113.6	>227.2	0
7	>227.2	>227.2	>227.2	113.6	>227.2	113.6	>227.2	0
8	28.4	113.6	>227.2	56.8	28.4	ND	56.8	80
9	>227.2	ND	>227.2	227.2	ND	ND	ND	0
10	>227.2	113.6	ND	113.6	ND	ND	ND	23
11	113.6	ND	56.8	7.1	14.2	ND	7.1	84
12	56.8	113.6	ND	56.8	ND	56.8	56.8	0
13	>227.2	>227.2	>227.2	113.6	>227.2	113.6	>227.2	0
14	22.7	7.1	28.4	7.1	14.2	3.5	0.8	16
15	7.1	14.2	56.8	3.5	3.5	3.5	0.8	40
16	3.5	7.1	56.8	3.5	7.1	7.1	3.5	4
17	>227.2	113.6	56.8	7.1	>56.8	ND	28.4	0
18	28.4	14.2	28.4	3.5	14.2	3.5	3.5	74
19	7.1	14.2	28.4	3.5	14.2	7.1	3.5	51
Tetracycline	0.3	0.3	ND	0.3	14.2	ND	>50	ND
Polymyxin B	0.7	0.7	ND	15.5	28.4	14.2	28.4	ND

ND: not determined.

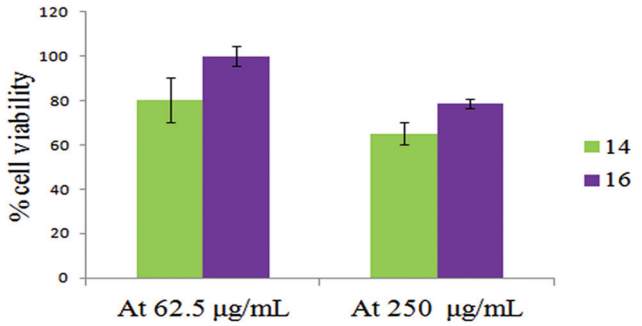

Fig. 2 Percentage viability of cells upon treatment with different concentrations of sequences based on the MTT assay. Error bars represent mean ± SD.

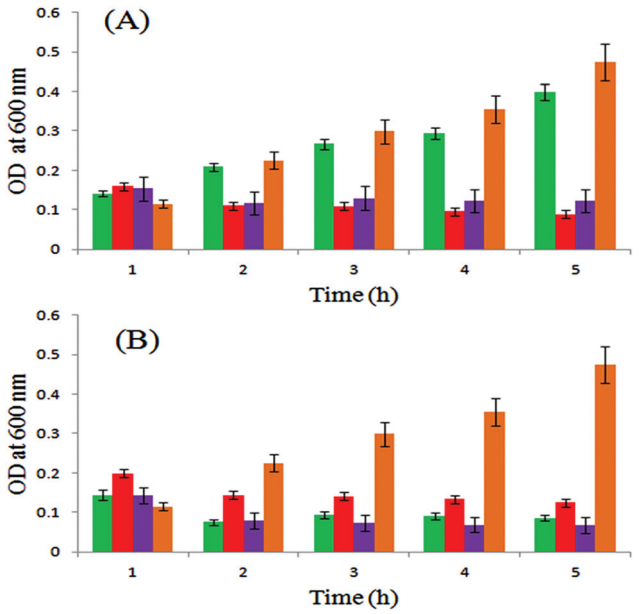

Fig. 3 Time dependent killing of MRSA upon treatment with different sequences at (A) MIC and (B) 4 × MIC. Sequences are presented as **14** (green bar), **15** (red bar), **16** (purple bar) and control (orange bar).

Sequence **14** was found to be less effective at MIC even up to 5 h. At 4 × MIC all three sequences inhibited bacterial growth from 2 h onwards keeping growth arrested till 5 h. However complete eradication of bacterial growth by any of the tested sequences was not observed up to 5 h. At 4 × MIC **16** exhibited the most potent inhibition of growth compared to **14** or **15**. Thus in line with HDCPs the designed sequences are capable of inhibiting bacterial growth within hours of initial interactions.

5. Calcein leakage

To examine the role of membrane interactions in the mode of action for designed sequences **14–19**, we first compared their membrane pore forming ability using artificial LUVs comprising bacterial mimic membranes with composition POPC : POPG [7 : 3, w/w]. For sequences **14** and **16**, graded release of encapsulated calcein dye upon increasing the concentration of sequences

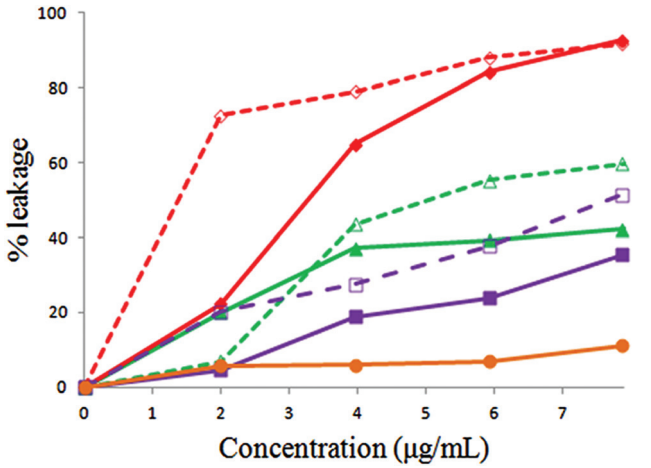

Fig. 4 Concentration-dependent leakage of encapsulated calcein dye from bacterial mimic POPC/POPG LUVs (180 µM) at pH 7.2 measured after 5 min of incubation with different concentrations of designed sequences. Sequences are presented as (▲) **14**, (◆) **15**, (■) **16**, (△) **17**, (◇) **18**, (⊟) **19** and (●) tetracycline.

was observed where at the highest concentration tested (7.87 µg mL^{-1}) partial leakage of vesicle contents was observed (Fig. 4). For **15** and **18** a rapid increase in fluorescent intensity due to a preferential pore forming ability was observed, where **18** caused a burst release of calcein dye at 1.99 µg mL^{-1} causing almost 72% leakage instantly. For sequences **17** and **19** moderate levels of leakage were observed where the maximum extent of leakage reached up to 60% and 51% respectively, at the highest concentration tested. These data make it clear that sequences with stearic acid conjugation lead to a better pore forming ability as compared to linoleic acid tagged sequences. Consistent with previous reports on HDCPs, the Trp–Trp dipeptide sequences **14** and **17** showed a preference to reside at the membrane interphase, causing relatively lower levels of calcein leakage.[34] Overall out of the active sequences, sequences **15** and **18** caused formation of large enough pores for complete leakage of encapsulated calcein dye whereas sequences **14** and **16** showed partial leakage and sequences **17** and **19** caused moderate levels of leakage. Standard antibiotic tetracycline showed less than 15% leakage up to the highest concentration tested.

6. Membrane depolarization

To study the mode of action on intact MRSA cells, a membrane depolarization experiment was performed. In this experiment if the sequences are able to alter membrane potential as a result of pore formation/membrane destabilization an increase in fluorescence intensity is observed. The data show concentration dependent effects and no perfect co-relation between MIC values and extent of membrane depolarization could be observed (Fig. 5). The changes in fluorescence were instant with maximum increase within 2 min after treatment at all concentrations. Only a 48% increase in fluorescence intensity was caused by active sequences **14** and **17** even up to a concentration of 19.2 µg mL^{-1}. Sequences **15**, **16**, **18** and **19** lead to significant depolarization of membrane potential leading to an almost

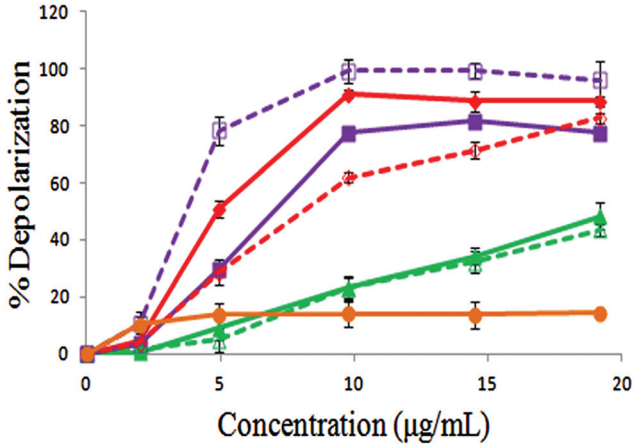

Fig. 5 Membrane depolarization ability of designed sequence. MRSA was grown to log phase (OD_{600} = 0.05) and treated with different concentrations of desired sequences. Sequences are presented as (▲) **14**, (◆) **15**, (■) **16**, (△) **17**, (◇) **18**, (□) **19** and (●) tetracycline.

78–96% increment in fluorescence at a concentration of 14.5 μg mL^{-1}. Concomitant with the depolarization experiment a PI uptake experiment was set up to evaluate if depolarization was a lethal event. The PI uptake data showed loss of viability upon treatment of MRSA with sequences at 19.2 μg mL^{-1} (data not shown here).

7. DNA binding

Antimicrobial potency of various classes of DNA binding agents is well reported in the literature.[37,38] We accessed DNA binding ability of sequences **14–19** as the role of spermidine in membrane translocation as well as DNA complexation is well known.[39] Sequences **14** and **16** showed binding with DNA (100 ng) causing retardation at 12.5 μg mL^{-1} where for **16** slight retardation was observed even at 6.25 μg mL^{-1} (Fig. 6). Sequence **15** showed excellent DNA binding ability with complete retardation at 3.12 μg mL^{-1}. Sequences **18** and **19** showed good DNA retardation ability with complete binding at 6.25 μg mL^{-1}. Noticeably Trp–Trp sequences **14** and **17** showed poor DNA complexation which may in part be ascribed to lower charge density in these sequences. However it was intriguing that DNA binding was influenced by overall structure of the sequences as Trp–Orn dipeptide containing sequences **15** and **18** showed the most potent DNA retardation ability as compared to Orn–Orn analogues **16** and **19**. Recently it was shown that a novel class of DNA minor groove binders based on benzophenone tetra-amide scaffolds showed strong DNA binding ability with membrane active bactericidal mode of action.[40] Therefore unexpectedly DNA binding was not directly involved with mode of action of this class of compounds.[41] On similar lines in the present study upon comparing DNA binding and antimicrobial potency (sequence **14** showed lesser DNA binding though was equipotent as **15**) it was evident that there were no direct correlations between DNA retardation and antimicrobial potency/mode of action.

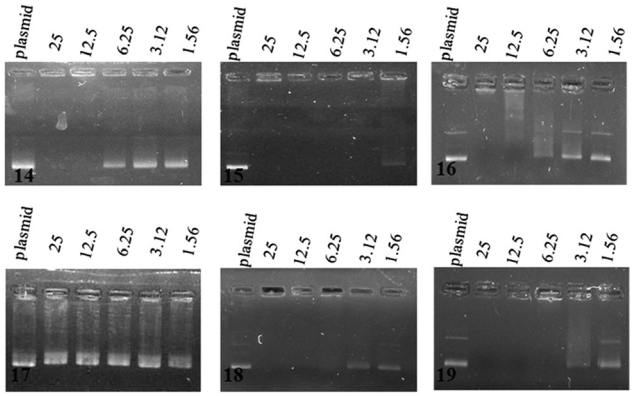

Fig. 6 Gel retardation assay, binding was assayed by the inhibitory effect of conjugates on the migration of DNA bands. Various amounts of conjugates were incubated with 100 ng of plasmid DNA at room temperature for 1 h and the reaction mixtures were applied to 1% agarose gel electrophoresis.

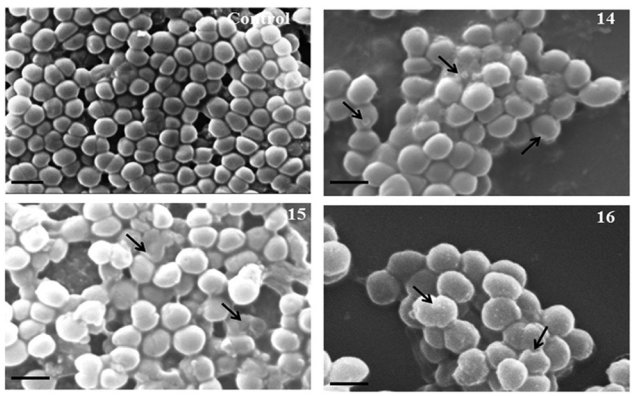

Fig. 7 Scanning electron microscopic images of MRSA (ATCC 33591) treated with sequences at 10 × MIC for 30 min. The bar in the image represents 1 μm.

8. Scanning electron microscopy

To have visual evidence for the membrane active mode of action, we incubated sequences **14**, **15** and **16** with MRSA at concentrations higher than MIC. Disintegration of bacterial membranes due to pore formation or surface swelling have been microscopically observed for membrane active HDCPs at concentrations higher than MIC.[42,43] Control MRSA cells exhibit a bright smooth appearance with an intact cell membrane (Fig. 7A).

Membrane damage and cellular debris as small and round structures were apparent upon treatment of MRSA with sequence **14** (Fig. 7B). In sequence **15** treated *S. aureus* cells, cellular protrusions as well as flattened cells due to complete leakage of cellular contents were visible (Fig. 7C). For sequence **16** deformed outer membranes were observed where surface blabbing was visible without much leakage of cellular contents (Fig. 7D). The appearance of such protrusions on the surface of *S. aureus* caused by HDCPs Gramicidin S and PGLa has recently been reported as well.[44] These data are in agreement with calcein leakage and membrane depolarization experiments where

sequence **15** caused cellular damage in the form of membrane disruption whereas **14** and **16** were found to show lesser leakage of encapsulated dye.

Overall the present study affords us sequences **14–19** with potent activity against a broad range of bacterial strains including MRSA. Upon dissecting the designed template to identify features responsible for activity and selectivity, we found that the cationic charge imparted to dipeptides by spermidine in sequences **1–3** was not sufficient *per se* to show bactericidal properties. Lipidation alone with neutral or negative charge in sequences **6**, **7**, **9** and **10** also led to low activity. With unit positive charge, lipidated sequences **8** and **11** exhibited improved activity though with compromised cell selectivity (Table 2). However conjugation of spermidine in sequences **14–19** improved potency as well as cell selectivity. With minimum +2 charges, lipidated sequences **14–19** showed a broad range of antibacterial activity.

Since the sequences show potent activity against MRSA, to have better insights into the mode of action of designed sequences we characterized their interactions with *S. aureus* mimic artificial membranes, intact MRSA and DNA.

Mode of action studies revealed a predominant role of the dipeptide sequence in initial binding, bactericidal kinetics and membrane disrupting abilities of designed sequences. For sequence **14**, low leakage causing ability, lower levels of membrane depolarization as well as reduced DNA binding ability make membrane destabilization a less probable mode of action at MIC. A slower bactericidal kinetics of **14** at MIC might as well be due to different modes of action operative at low concentrations. Slower bactericidal kinetics has previously been reported for HDCP mimics interfering with vital functions in bacterial cells other than membrane disruption.[45] However in SEM studies at concentrations 10 × MIC cellular debris and diffused outer bacterial membranes were evident for **14** potentiating a membrane disruptive mode of action (Fig. 7B). Sequence **15** showed faster leakage of calcein along with membrane depolarization, rapid killing kinetics and excellent DNA binding ability. Therefore this sequence showed clean membrane perturbing mode of action at MIC as well as higher concentrations as was evidenced in SEM images of the treated MRSA (Fig. 7C). Sequence **16** with rapid bactericidal kinetics, good DNA binding ability caused appreciable damage to membrane potential in MRSA at the tested concentrations, however moderate levels of leakage causing ability showed that either transient pores were formed or the pores were not large enough to cause leakage of calcein which is evident by the surface blabbing observed in SEM studies. A low leakage causing ability in spite of potent membrane depolarization has previously been reported for analogues of HDCP indolicidin.[46]

Conclusion

In summary, using simple chemistry and economically viable building blocks FFAs (linoleic acid/stearic acid), Trp, Orn and spermidine, we obtained 6 active sequences with a broad range of activity against Gram-positive as well as Gram-negative bacterial strains including clinically relevant pathogen MRSA. Sequences **14** and **16** showed excellent cell selectivity and membrane perturbing mode of action at concentrations higher than MIC. These sequences were also able to alter the electrophoretic mobility of DNA which although was not directly related to activity may as well be responsible for further enhanced potency of these sequences due to intracellular mode of action. The structure–activity work in this study paves the way for the design of optimized FFAs based peptidomimetics with spermidine/spermine conjugated with different combinations of amino acids which is currently in progress in our laboratory.

Experimental section

Materials

Fmoc-protected amino acids and resins were purchased from Novabiochem. Dimethylamino pyridine (DMAP), *N*,*N*-diisopropylcarbodiimide (DIPCDI), *N*-hydroxybenzotrizole (HOBt), diisopropyl ethylamine (DIPEA), *N*-methyl pyrrolidinone (NMP), piperidine, trifluoroethanol (TFE), trifluoroacetic acid (TFA), triisopropyl silane (TIS), calcein and 3,3′-dipropylthiadicarbocyanine iodide ($DiSC_35$) were obtained from Sigma Chemical Co. 1-Palmitoyl-2-oleoyl-*sn*-glycero-3-phosphocholine (POPC) and 1-palmitoyl-2-oleoyl-*sn*-glycero-3-phospho-(1′-*rac*-glycerol) (sodium salt) (POPG) were purchased from Avanti Polar Lipids. Dulbecco's modified Eagles' medium-high glucose (DMEM), antibiotic/antimycotic solutions, heat inactivated fetal bovine serum (FBS), trypsin from porcine pancreas and 3-(4,5-dimethyl-2-thiazolyl)-2,5-diphenyl-2*H*-tetrazolium bromide (MTT) were obtained from Sigma Aldrich Chemical Company. All solvents used for the purification were of HPLC grade and obtained from Merck, Germany. Dimethylformamide (DMF) and dichloromethane (DCM) were obtained from Merck India. DMF was double distilled prior to use.

Synthesis and purification of sequences

The dipeptides were synthesized on 2-chlorotrityl chloride resin as a solid support using Fmoc chemistry as reported previously.[47] The terminal amino group of dipeptides was Boc protected on a solid support before cleavage from the resin under mild conditions ($TFE : CH_3COOH : CH_2Cl_2$ cocktail, 1 : 1 : 8) to retain Boc groups. The cleaved dipeptides were coupled with N^1,N^4-bis(boc)spermidine (SIGMA) using HOBt and DIPCDI in dry tetrahydrofuran under a N_2 atmosphere at 0 °C for 30 min followed by 18 h at rt as reported previously.[48] The obtained product was dissolved in $CHCl_3$ (15 mL) and washed with 1% aqueous $NaHCO_3$ (50 mL), 1% aqueous HCl (50 mL), and brine (50 mL). The organic layer was dried over anhydrous Na_2SO_4 and concentrated under reduced pressure to give crude dipeptide spermidine conjugates. Boc groups were removed from the conjugates using 50% TFA in CH_2Cl_2 to give sequences **1–3**. On a solid support N-terminal end tagging of dipeptides was achieved by coupling 4 equiv. of 3-(4-hydroxyphenyl)-propionic acid (HPPA)/linoleic acid/stearic acid overnight with HOBt and DIPCDI. The Kaiser test was performed to check completion of reactions on a solid support.[49] The N-terminal tagged di-peptidomimetics were cleaved from a solid support under two different conditions. For synthesis of **4–11**, cleavage was effectuated using 50% TFA in DCM. For synthesis of **12–19**, cleavage was

performed under mild conditions (TFE : CH_3COOH : CH_2Cl_2 cocktail 1 : 1 : 8). Further Boc protected N-terminal tagged conjugates were coupled with N^1,N^4-bis(boc) spermidine as described for dipeptides earlier in the text. Finally Boc groups were removed with 50% TFA resulting in sequences **12–19**. Synthesized sequences were purified using an RP-HPLC column (7.8 × 300 mm, 125 Å, 10 μm particle size) with either gradients of 10 to 90% buffer 2 where buffer 1 was water (0.05% TFA) and buffer 2 was acetonitrile (0.05% TFA) over 45 min or 30 to 100% buffer 2 gradients were run over 45 min where buffer 1 was water (0.1% TFA) and buffer 2 was acetonitrile (0.1% TFA). The correct sequences after purification were confirmed by LC-MS/MS (Quattro micro API, Waters), LC-ESI-HRMS on UHPLC (Dionex, Germany) and LTQ Orbitrap XL (Thermo Fisher Scientific, USA) mass determination and ^{1}H NMR. Mass spectra, analytical HPLC traces and ^{1}H NMR data of representative sequences are provided in supplementary files.

Antibacterial activity

Antibacterial activity of designed sequences was evaluated using a modification of the serial broth dilution method as reported previously.[50] Bacterial strains used in this study were as follows, *E. coli* (ATCC 11775), *P. aeruginosa* (ATCC 25668), *A. baumannii* (ATCC 19606), *S. aureus* (ATCC 29213), *E. faecalis* (ATCC 7080), *B. subtilis* (ATCC 6633) and methicillin resistant *S. aureus* (ATCC 33591). The inoculums were prepared from mid-log phase bacterial cultures. Each well of the first 11 columns of a 96-well polypropylene micro titre plate (SIGMA) was inoculated with 100 μL of approximately 10^5 CFU mL^{-1} of bacterial suspension per mL of Mueller-Hinton broth (MHB, DIFCO). Then 11 μL of serially diluted test sequences in 0.001% acetic acid and 0.2% bovine serum albumin (SIGMA) over the desired concentration range was added to the wells of micro titre plates. The micro titre plates were incubated overnight with agitation (200 rpm) at 37 °C. After 18 h absorbance was read at 630 nm. Cultures (approximately 10^5 CFU mL^{-1}) without test sequences were used as a positive control. Un-inoculated MHB was used as a negative control. Tests were carried out in duplicate on three different days. Minimum inhibitory concentration (MIC) is defined as the lowest concentration of test sequences that completely inhibits growth. For comparison peptide antibiotic polymyxin B and tetracycline were also assayed under identical conditions.

Hemolytic activity

Hemolytic activity assay was done as described previously.[51] Briefly, 100 μL of fresh hRBC suspension 4% v/v in PBS (35 mM phosphate buffer, 150 mM NaCl) was placed in a 96-well plate. After incubation of the test sequences (100 μL) in the erythrocyte solution for 1 h at 37 °C, the plates were centrifuged and the supernatant (100 μL) was transferred to fresh 96-well plates. Absorbance was read at 540 nm using an ELISA plate reader (Molecular Devices). Percent hemolysis was calculated using the following formula:

$$\% \text{ hemolysis} = 100[(A - A_0)/(A_t - A_0)]$$

where A represents absorbance of sample wells at 540 nm and A_0 and A_t represent zero percent and 100% hemolysis determined in PBS and 1% Triton X-100, respectively.

Cytotoxicity

To assess cell viability, the MTT assay was performed as described previously.[52] HaCaT keratinocytes, 3000 cells per well, were seeded in 96-well plates in DMEM HAMS F12 media supplemented with 10% serum (FBS) to grow overnight. The next day media were aspirated and fresh incomplete media were added (50 μL per well). To the wells serial two-fold dilutions of different test sequences (50 μL) were added and the plates were incubated at 37 °C with 5% CO_2 for 18 h. After 18 h the media were aspirated and 100 μL of MTT solution was added to each well. The plates were further incubated for 4 h in CO_2 at 37 °C. After 4 h the MTT-containing medium was removed by aspiration. The blue formazan product generated was dissolved by the addition of 100 μL of 100% DMSO per well. The plates were then gently swirled for 2–3 min at room temperature to dissolve the precipitate. The absorbance was monitored at 540 nm. Percentage viability was calculated based on the following formula:

$$\% \text{ cell viability} = (A/A_{\text{control}}) \times 100$$

where A represents sample absorbance at a given concentration and A_{control} represents untreated cells. The experiment was repeated thrice and results are given as mean ± SD.

Bactericidal kinetics

Overnight cultures of methicillin resistant *S. aureus* (ATCC 33591) were grown in fresh MHB up to log phase. For determining the time course of killing activity 100 μL of fresh MHB was added to all wells of the 96 well-plate. Then 90 μL of approximately 10^5 CFU mL^{-1} were added to the wells of the 96-well plate (4 wells for a single concentration). Then 10 μL of appropriate concentrations of test sequences corresponding to MIC and 4 × MIC were added to the wells. The plates were incubated at 37 °C at 200 rpm. Absorbance of the plates was read at 600 nm at various time points at 0, 1, 2, 3, 4 and 5 h. The experiment was repeated on three different days and values are plotted as mean ± SD.

Calcein leakage

The ability of designed sequences **14–19** to cause leakage from artificial LUVs composed of bacterial mimic membrane (POPC/POPG) was accessed as described previously.[53,54] Briefly, desired mixtures of the lipids POPC/POPG (7 : 3, w/w) were dissolved in a 2 mL chloroform–methanol mixture in a 150 mL round bottom flask. The solvent was removed under a stream of nitrogen and the lipid film obtained was lyophilized overnight to remove any traces of organic solvent. The dry lipid films were rehydrated with 10 mM Tris-HCl [70 mM calcein, 150 mM NaCl, 0.1 mM EDTA]. The liposome suspension obtained after rehydration was freeze thawed for five cycles and extruded 16 times through two stacked

polycarbonate filters (Mini extruder, Avanti Polar Lipids). Free calcein was removed by passing the liposome suspension through a Sephadex G-50 column at 23 °C and eluting with a buffer containing 10 mM Tris-HCl [150 mM NaCl, 0.1 mM EDTA]. After passing the liposome through a Sephadex G-50, liposome diameter was measured by dynamic light scattering using a Zetasizer Nano ZS (Malvern Instruments). The average diameter of LUVs was found to be in the range of 90–110 nm. Different concentrations of test sequences were incubated with POPC/POPG LUVs for 5 min before exciting the samples. Leakage was monitored by measuring the fluorescence intensity at an emission wavelength of 520 nm upon excitation at 490 nm on a model Fluorolog (Jobin Yuvon, Horiba) spectrofluorimeter. A slit width of 3 nm was used for both excitation and emission. Percentage dye leakage was calculated using the formula

$$\% \text{ dye leakage} = 100[(F - F_0)/(F_t - F_0)]$$

where F is the fluorescence intensity achieved by addition of different concentrations of sequences. F_0 and F_t are fluorescence intensities in buffer and with Triton X-100 (20 μL of 10% solution) respectively. All measurements were made in duplicate and less than 4% deviation was obtained in the data points. A phosphate assay was performed to determine the concentration of lipids for the leakage experiment.[55]

Membrane depolarization

For the evaluation of membrane depolarization a previously defined method was used.[56] Briefly, overnight grown MRSA was subcultured into MHB for 2–3 h at 37 °C to obtain midlog phase cultures. The cells were centrifuged at 4000 rpm for 10 min at 25 °C, washed, and re-suspended in respiration buffer (5 mM HEPES, 20 mM glucose, pH 7.4) to obtain a diluted suspension of $OD_{600} \approx 0.05$. A membrane potential-sensitive dye, 3,3′-dipropylthiadicarbocyanine iodide ($DiSC_35$), 0.18 μM (prepared in DMSO) was added to a 500 μL aliquot of the re-suspended cells and allowed to stabilize for 1 h. Baseline fluorescence was acquired using a Fluorolog (Jobin Yuvon, Horiba) spectrofluorometer by excitation at 622 nm and emission at 670 nm. A bandwidth of 5 nm was employed for excitation and emission. Subsequently, increasing concentrations of test sequences between 2 and 19.2 μg mL^{-1} were added to the stabilized cells and the increase of fluorescence on account of the dequenching of $DiSC_35$ dye was measured after every 2 min to obtain the maximal depolarization. Percent depolarization was calculated by using the formula

$$\% \text{ depolarization} = (F - F_0)/(F_m - F_0) \times 100$$

where F is the fluorescence intensity 2 min after addition of sequences, F_0 is the initial basal fluorescence intensity, and F_m is the maximum fluorescence intensity obtained after addition of 10 μg mL^{-1} gramicidin. Percent depolarization mean ± SD of two independent experiments was plotted *versus* increasing concentrations of different sequences.

DNA binding assay

Gel retardation experiments were performed as described previously.[54,57] Briefly, 100 ng of plasmid DNA (pBluescript II SK+) was mixed with increasing amounts of test sequences **14–19** in 20 μL of binding buffer (5% glycerol, 10 mM Tris-HCl, pH 8.0, 1 mM EDTA, 1 mM dithiothreitol, 20 mM KCl, and 50 μg mL^{-1} bovine serum albumin). Reaction mixtures were incubated at room temperature for 1 h. Subsequently, 4 μL of native loading buffer was added (10% Ficoll 400, 10 mM Tris-HCl, pH 7.5, 50 mM EDTA, 0.25% bromophenol blue, and 0.25% xylene cyanol), and a 20 μL aliquot subjected to 1% agarose gel electrophoresis in 0.5× Tris borate–EDTA buffer (45 mM Tris-borate and 1 mM EDTA, pH 8.0). The gels were run for 1.5 h at 80 V and visualized with ethidium bromide. The plasmid DNA was purchased from Stratagene and was used as such without further purification.

Scanning electron microscopy

For electron microscopy samples were prepared as described previously.[58] Briefly, freshly inoculated methicillin resistant *S. aureus* (ATCC 33591) was grown on MHB up to an OD_{600} of 0.5 (corresponding to 10^8 CFU mL^{-1}). Bacterial cells were then spun down at 4000 rpm for 15 min, washed thrice in PBS (20 mM, 150 mM NaCl) and re-suspended in an equal volume of PBS. The cultures were then incubated with test sequences **14**, **15** or **16** at 10 × MIC for 30 min. Controls were run in the absence of sequences. After 30 min, the cells were spun down and washed with PBS thrice. For cell fixation the washed bacterial pallet was re-suspended in 1 mL of 2.5% glutaraldehyde in PBS and was incubated at 4 °C for 4 h. After fixation, cells were spun down and washed with PBS twice. Further the samples were dehydrated in series of graded ethanol solutions (30% to 100%), and finally dried in desiccators under a vacuum. An automatic sputter coater (Polaron OM-SC7640) was used for coating the specimens with 20 nm gold particles. Then samples were viewed *via* a scanning electron microscope (EVO 40, Carl Zeiss, Germany).

Acknowledgements

This work was financially supported by a Council of Scientific and Industrial Research (CSIR) network project NWP-013. We thank Dr Souvik Maiti and Dr Kausik Chakraborty for useful discussions and instrumentation facility. We acknowledge the Analytical Instrumental Research Facility at Jawahar Lal Nehru University, Delhi, India for providing us scanning electron microscopic facility. Dr V. Sabareesh and Richa Guleria are acknowleged for help in ESI-HR-MS data acquisition. The author S.J. is thankful to CSIR, New Delhi, India, for the award of SRF.

References

1 S. B. Levy and B. Marshall, *Nat. Med.*, 2004, **10**, 122.
2 J. Davies and D. Davies, *Microbiol. Mol. Biol. Rev.*, 2010, **74**, 417.
3 A. Opar, *Nat. Rev. Drug Discovery*, 2007, **6**, 943.
4 R. E. W. Hancock and H. G. Sahl, *Nat. Biotechnol.*, 2006, **24**, 1551.

5 M. Zasloff, *Nature*, 2002, **415**, 389.
6 J. He, D. K. Yarbrough, J. Kreth, M. H. Anderson, W. Shi and R. Eckert, *Antimicrob. Agents Chemother.*, 2010, **54**, 2143.
7 S. E. Blondelle and K. Lohner, *Curr. Pharm. Des.*, 2010, **28**, 3204.
8 P. W. Latham, *Nat. Biotechnol.*, 1999, **17**, 755.
9 M. B. Strom, B. E. Haug, M. L. Skar, W. Stensen, T. Stiberg and J. S. Svendsen, *J. Med. Chem.*, 2003, **46**, 1567.
10 B. Ding, N. Yin, Y. Liu, J. C. Garcia, R. Evanson, T. Orsak, M. Fan, G. Turin and P. B. Savage, *J. Am. Chem. Soc.*, 2004, **126**, 13642.
11 J. N. Chin, M. J. Rybak, C. M. Cheung and P. B. Savage, *Antimicrob. Agents Chemother.*, 2007, **51**, 1268.
12 I. S. Radzishevsky, S. Rotem, D. Bourdetsky, S. Navon-Venezia, Y. Carmeli and A. Mor, *Nat. Biotechnol.*, 2007, **25**, 657.
13 F. Zaknoon, H. Sarig, S. Rotem, L. Livne, A. Ivankin, D. Gidalevitz and A. Mor, *Antimicrob. Agents Chemother.*, 2009, **53**, 3422.
14 N. Srinivas, K. Moehle, K. A. Hadeed, D. Obrecht and J. A. Robinson, *Org. Biomol. Chem.*, 2007, **5**, 3100.
15 N. P. Chongsiriwatana, T. M. Miller, M. Wetzler, S. Vakulenko, A. J. Karlsson, S. P. Palacek, S. Mobashery and A. E. Barron, *Antimicrob. Agents Chemother.*, 2011, **55**, 417.
16 A. Makovitzki, D. Avrahami and Y. Shai, *Proc. Natl. Acad. Sci. U. S. A.*, 2006, **103**, 15997.
17 W. Kamysz, C. Silvestri, O. Cirioni, A. Giacometti, A. Licci, A. Della Vittoria, M. Okroj and G. Scalise, *Antimicrob. Agents Chemother.*, 2007, **51**, 354.
18 K. Igarashi and K. Kashiwagi, *Biochem. Biophys. Res. Commun.*, 2000, **271**, 559.
19 A. Shrestha, D. Sil, S. S. Malladi, H. J. Warshakoon and S. A. David, *Bioorg. Med. Chem. Lett.*, 2009, **19**, 2478.
20 X. Bi, C. Lopez, C. J. Bacchi, D. Rattendi and P. M. Woster, *Bioorg. Med. Chem. Lett.*, 2006, **16**, 3229.
21 B. K. Verlinden, J. Niemand, J. Snyman, S. K. Sharma, R. J. Beattie, P. M. Woster and L. M. Birkholtz, *J. Med. Chem.*, 2011, **54**, 6624.
22 T. Yildirim, K. Bilgin, G. Y. Ciftci, E. T. Ecik, E. Senkuytu, Y. Uluda, L. Tomak and A. Kilic, *Eur. J. Med. Chem.*, 2012, **52**, 213.
23 R. A. Casero Jr. and P. M. Woster, *J. Med. Chem.*, 2009, **52**, 4551.
24 A. Liberska, A. Lilienkampf, A. U. Broceta and M. Bradley, *Chem. Commun.*, 2011, **47**, 12774.
25 D. R. Drake, K. A. Brogden, D. V. Dawson and P. W. Wertz, *J. Lipid Res.*, 2008, **49**, 4.
26 M. Farrington, N. Brenwald, D. Haines and E. Walpole, *J. Med. Microbiol.*, 1992, **36**, 56.
27 C. Q. Sun, C. J. O'Connor and A. M. Roberton, *FEMS Immunol. Med. Microbiol.*, 2003, **36**, 9.
28 P. A. Desbois and V. J. Smith, *Appl. Microbiol. Biotechnol.*, 2010, **85**, 1629.
29 C. J. Zheng, J. S. Yoo, T. G. Lee, H. Y. Choc, Y. H. Kim and W. G. Kim, *FEBS Lett.*, 2005, **579**, 5157.
30 M. Vaara, J. Fox, G. Loidl, O. Siikanen, J. Apajalahti, F. Hansen, N. Frimodt-Moller, J. Nagai, M. Takano and T. Vaara, *Antimicrob. Agents Chemother.*, 2008, **52**, 3229.
31 J. N. Steenbergen, J. Alder, G. M. Thorne and F. P. Tally, *J. Antimicrob. Chemother.*, 2005, **55**, 283.
32 M. P. C. Mulder, J. A. W. Kruijtzer, E. J. Breukink, J. Kemmink, R. J. Pieters and R. M. J. Liskamp, *Bioorg. Med. Chem.*, 2011, **19**, 6505.
33 H. Sarig, S. Rotem, L. Ziserman, D. Danino and A. Mor, *Antimicrob. Agents Chemother.*, 2008, **52**, 4308.
34 D. I. Chan, E. J. Prenner and H. J. Vogel, *Biochim. Biophys. Acta*, 2006, **1758**, 1184.
35 G. S. Bisht, D. S. Rawat, A. Kumar, R. Kumar and S. Pasha, *Bioorg. Med. Chem. Lett.*, 2007, **17**, 4343.
36 Y. Chen, M. T. Guarnieri, A. I. Vasil, M. L. Vasil, C. T. Mant and R. S. Hodges, *Antimicrob. Agents Chemother.*, 2007, **51**, 1398.
37 J. A. Kaizerman, M. I. Gross, Y. Ge, S. White, W. Hu, J. X. Duan, E. E. Baird, K. W. Johnson, R. D. Tanaka, H. E. Moser and R. W. Burli, *J. Med. Chem.*, 2003, **46**, 3914.
38 A. I. Khalaf, A. H. Ebrahimabadi, A. J. Drummond, N. G. Anthony, S. P. Mackay, C. J. Suckling and R. D. Waigh, *Org. Biomol. Chem.*, 2004, **2**, 3119.
39 J. G. Delcros, S. Tomasi, S. Duhieu, M. Foucault, B. Martin, M. Roch, V. Eifler-Lima, J. Renault and P. Uriac, *J. Med. Chem.*, 2006, **49**, 232.
40 S. K. Vooturi, C. M. Cheung, M. J. Rybak and S. M. Firestine, *J. Med. Chem.*, 2009, **52**, 5020.
41 S. K. Vooturi, M. B. Dewal and S. M. Firestine, *Org. Biomol. Chem.*, 2011, **9**, 6367.
42 I. L. Exposito, L. Amigo and I. Recio, *Biochim. Biophys. Acta*, 2008, **1778**, 2444.
43 A. J. Hyde, J. Parisot, A. McNichol and B. B. Bonev, *Proc. Natl. Acad. Sci. U. S. A.*, 2006, **103**, 19896.
44 M. Hartmann, M. Berditsch, J. Hawecker, M. F. Ardakani, D. Gerthsen and A. S. Ulrich, *Antimicrob. Agents Chemother.*, 2010, **54**, 3132.
45 S. Rotem, I. S. Radzishevsky, D. Bourdetsky, S. N. Venezia, Y. Carmeli and A. Mor, *FASEB J.*, 2008, **22**, 2652.
46 Y. H. Nan, J. K. Bang and S. Y. Shin, *Peptides*, 2009, **30**, 832.
47 K. Barlos, O. Chatzi, D. Gatos and G. Stavropoulos, *Int. J. Pept. Protein Res.*, 1991, **37**, 513.
48 W. H. Chen, X. B. Shao, R. Moellering, C. Wennersten and S. L. Regen, *Bioconjugate Chem.*, 2006, **17**, 1582.
49 E. Kaiser, R. L. Colescott, C. D. Bossinger and P. I. Cook, *Anal. Biochem.*, 1970, **34**, 595.
50 M. A. Wikler, D. E. Low, F. R. Cockerill, D. J. Sheehan, W. A. Craig, F. C. Tenover and M. L. Dudley, Methods for dilution antimicrobial susceptibility tests for bacteria that grow aerobically: approved standard-seventh edition (2006) CLSI (formerly NCCLS) M7-A7.
51 M. Sharma, P. Joshi, N. Kumar, S. Joshi, R. K. Rohilla, N. Roy and D. S. Rawat, *Eur. J. Med. Chem.*, 2011, **46**, 480.
52 L. Schmidtchen, G. Ringstad, H. Kasetty, M. W. Mizuno, M. Rutland and M. Malmsten, *Biochim. Biophys. Acta*, 2011, **1808**, 1081.
53 L. Zhang, A. Rozek and R. E. W. Hancock, *J. Biol. Chem.*, 2001, **276**, 35714.
54 S. Joshi, G. S. Bisht, D. S. Rawat, A. Kumar, R. Kumar, S. Maiti and S. Pasha, *Biochim. Biophys. Acta*, 2010, **1798**, 1864.
55 G. R. Bartlett, *J. Biol. Chem.*, 1959, **234**, 466.
56 P. N. Domadia, A. Bhunia, A. Ramamoorthy and S. Bhattacharjya, *J. Am. Chem. Soc.*, 2010, **132**, 18417.
57 S. T. Yang, J. Y. Lee, H. J. Kim, Y. J. Eu, S. Y. Shin, K. S. Hahm and J. I. Kim, *FEBS J.*, 2006, **273**, 4040.
58 M. Singh and K. Mukhopadhyay, *Antimicrob. Agents Chemother.*, 2011, **55**, 1920.

